World Electric Vehicle Journal

MDPI

Article

A Predictive Cabin Conditioning Strategy for Battery Electric Vehicles

Patrick Schutzeich [1,*], Stefan Pischinger [1], David Hemkemeyer [2], Kai Franke [1] and Paul Hamelbeck [1]

[1] Chair of Thermodynamics of Mobile Energy Conversion Systems (TME), RWTH Aachen University, Forckenbeckstraße 4, 52074 Aachen, Germany
[2] FEV, Neuenhofstraße 181, 52078 Aachen, Germany
* Correspondence: schutzeich@tme.rwth-aachen.de

Abstract: This paper is based on the work presented at EVS36 in Sacramento. The core of the work deals with the cabin climate control of battery electric vehicles (BEV) using model predictive control (MPC) approaches. These aim to reduce the energy demand for cabin air conditioning while maintaining comfort and air quality. The first step briefly overviews model predictive control approaches and the respective fundamentals. Afterward, the modeling for the system dynamics is explained. The challenge for the system model considering humid air is discussed, and the first implementation method is presented. With the added equations for the air quality and humidity, a logic to prevent window fogging was developed to improve safety. Ultimately, model-in-the-loop (MiL) investigations identified an energy-saving potential of up to 15.4% for cold and 39.7% for hot conditions compared to a rule-based strategy. In addition, the investigations carried out showed that it was also possible to improve indoor comfort by specifically influencing the air quality and humidity. Together with the safety criteria introduced to prevent window fogging, it was possible to present a strategy that can significantly improve thermal management for the cabin in modern BEVs.

Keywords: BEV; air conditioning; control system; energy efficiency; MPC; cabin comfort; air quality

Citation: Schutzeich, P.; Pischinger, S.; Hemkemeyer, D.; Franke, K.; Hamelbeck, P. A Predictive Cabin Conditioning Strategy for Battery Electric Vehicles. *World Electr. Veh. J.* **2024**, *15*, 224. https://doi.org/10.3390/wevj15060224

Academic Editors: Joeri Van Mierlo and Genevieve Cullen

Received: 21 March 2024
Revised: 29 April 2024
Accepted: 14 May 2024
Published: 22 May 2024

1. Introduction

At the UN Climate Change Conference in September 2015, 197 countries committed to limiting global warming to 1.5 °C compared to the pre-industrial age [1]. The steps required to achieve this were set out by the European Union (EU) in its Green Deal. This postulates the goal of reaching climate neutrality by 2050 [2]. Individual countries in Europe have set even stricter targets. The German government wants to achieve greenhouse gas neutrality by 2045. This is linked to the planned reduction of relevant emissions by 65% compared to 1990 levels until 2030 [3]. Many Europeans currently support the measures presented to achieve the targets [4].

Nevertheless, the planned projects will majorly impact mobility in Europe. In addition to revising CO_2 restrictions, investments in charging infrastructure are also intended to boost emission-free mobility in Europe [2,5]. In Germany, electric and fuel cell vehicles are also specifically promoted via an environmental bonus. In addition, the number of public charging points is to be increased to 1 million by 2030. The measures aim to bring up to 15 million fully electric cars onto German roads by 2030 [6].

Even if the development of the registrations for electrified vehicles within Europe (EU-27) looks very positive at first glance, they still fall short of expectations. Figure 1 shows these for the years 2010 to 2021. The number of battery electric vehicles (BEV) and plug-in hybrid electric vehicles has increased from around 7000 in 2011 to around 1.7 million in 2021 for the EU-27 states [7]. Despite the positive development, the share of electric vehicles will have to rise further to meet the EU's self-imposed targets. Customer acceptance and enthusiasm for electrified mobility must be further improved to achieve

this. In particular, the range must be increased and charging times shortened to generate new purchasing impulses [8].

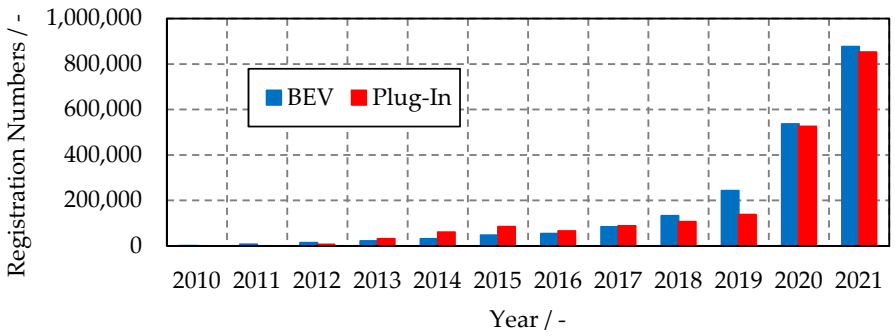

Figure 1. New registrations of electric cars, EU-27 (2011–2021) [7].

In particular, the cabin conditioning of BEVs strongly impacts the achievable driving range under hot and cold ambient conditions. In winter, heating the cabin can cause the achievable driving distance to deviate by up to 50% from the manufacturer's specifications [9–11]. The losses for short trips can increase to up to 70% [12,13]. This is mainly because the energy required must be taken directly from the battery to provide the necessary heating or cooling performance [14,15]. This further underlines the importance of an optimized thermal management strategy for the cabin conditioning of BEVs. The challenge is to minimize the energy required for cabin air conditioning while at the same time meeting the comfort requirements of the occupants.

One way of further developing the control system for heating and cooling the vehicle cabin is to use model predictive control approaches. These allow the control variables for a planned route to be calculated in advance and aim to achieve the desired interior temperature while minimizing energy consumption. A large amount of current research is mainly aimed at reducing energy requirements. Other important aspects, such as indoor air quality, passenger comfort, and humidity, should be considered. Nevertheless, using MPC has made it possible to demonstrate initial energy-saving potential [16–18]. This paper presents a model predictive control strategy for the energy-efficient air conditioning of BEVs. In this approach, the air quality is measured regarding CO_2 concentration, and comfort inside the cabin is ensured by evaluating the equivalent temperature. In addition to the already published investigations [19,20], a method is presented to consider air humidity and thus actively avoid windshield fogging. Comparable studies on model predictive control of cabin conditioning taking into account humidity were also presented in [21]. In contrast to the approaches presented there, using the acados framework [22–24] ensures that the MPC is suitable for vehicle operation. This was already demonstrated in the CEVOLVER project [25–28]. Furthermore, combining the consideration of humid air and the evaluation of the influence of the radiant surfaces through the equivalent temperature (EQT) ensures that many vehicle configurations can be investigated.

This publication focuses on expansion of the MPC by introducing a strategy to prevent window fogging. First, the basic principles of MPC controls are explained. Then, the necessary adaptations for implementing air humidity are presented. Finally, the first investigations on the control strategy are shown and evaluated. This conference paper is based on a contribution to the EVS 36 [29] and was significantly reworked for the publication within this journal. With the additions made, this publication addresses the challenges associated with humid air and shows ways in which these can be overcome efficiently and safely through an MPC strategy.

2. Fundamentals of the Model Predictive Control Approach

In engineering, model predictive control (MPC) is gaining popularity. It offers mathematical solutions for optimizing precisely formulated problems. Different decisions, consequences, and constraints can be considered to determine a suitable operating strategy

for a defined system. The objective evaluation criterion is expressed by a cost function J and minimized [30]. This section briefly discusses the basic principles of MPC approaches. Afterward, the scope and specifications of the control strategy are explained.

This paper uses an MPC as an online optimization that determines the required control signals at a defined time step $\Delta\tau_s$. The optimization problem must be set up to satisfy the real-time constraints. This implies that the time between the initiation of the optimization process and the output of the control signals must be correspondingly short to the selected step size $\Delta\tau_s$ [30–32]. The standard formulation of this optimization problem is presented in the following equations:

$$\min_{c} J(c) = \sum_{k=0}^{N-1} l(x(k), u(k), k) \text{ Cost function} \quad (1)$$

under consideration of the following:

$$x(k+1) = f(x(k), u(k), k), k = 0, \ldots, N-1 \text{ System dynamic} \quad (2)$$

$$h(x(k), u(k), k) \leq 0, k = 0, \ldots, N-1 \text{ Inequality constraint} \quad (3)$$

$$G(x(k), u(k), k) = 0, k = 0, \ldots, N-1 \text{ Equality constraint} \quad (4)$$

$$x(0) = x_0 \text{ Initial conditions} \quad (5)$$

The complexity of the stated problem does not allow the optimization to be solved efficiently by analytical methods. For this reason, as is typical for many other technical applications, numerical solution methods are used [30]. A direct solution method was selected, characterized by the fact that the optimization problem is initially discretized on a defined time domain and can then be solved with static optimization methods. This solution method is widely used in MPC applications [30,33,34]. The multi-shooting method was chosen from the direct methods for its high accuracy while being well suited for real-time optimization [30,34]. This solution method includes a discrete dynamic optimization problem whose formulation is shown in Equations (1)–(5) [30]. This specific form of problem formulation is also known as non-linear programming (NLP) and is often used in this context. It considers the starting conditions of the system and the system dynamics, which a mathematical model and the constraints represent. These can be utilized, for example, to limit the state or control variables [35].

Cabin conditioning can be defined as a nonlinear multivariable system under constraints. For these kinds of systems, the nonlinear MPC approach is suitable. Considering the control objectives, the problem is solved on a fixed prediction horizon N_p. These include achieving a target temperature in the interior and minimizing the energy demand in the case of cabin air conditioning. For the entire prediction horizon, the vectors for the control variables are calculated for each time step. However, only the vector with the values for the current time is passed to the system to be controlled. After one time step $\Delta\tau_s$, the controller is reinitialized, and the optimization problem is solved again. It also shifts the prediction horizon at this time, which is why it is also called the sliding prediction horizon [35].

The acados [24] framework was used to implement the MPC in MATLAB Simulink. This approach has already been used for applications of nonlinear MPC in the field of powertrain conditioning, and its functionality has been proven [36].

3. Realization of the MPC Control Strategy in a Model-in-the-Loop (MiL) Environment

After a short introduction to the basics of MPC, this section describes its implementation in MATLAB Simulink. For this purpose, the structure of the model-in-the-loop environment will be discussed first. Subsequently, the system dynamics modeling is explained for the cabin conditioning, and a method to include air humidity is presented.

3.1. Structure of the MiL Environment

The MiL environment consists of three core elements—the plant model, the prediction function, and the MPC. The plant model represents the system behavior outside the control structure and provides important state variables to the MPC and the prediction function. The sensor interfaces replace the plant model during later implementation in the vehicle and are no longer needed. For this purpose, the interface must be adapted accordingly. The plant model contains the same mathematical descriptions as the MPC for the simulative considerations presented in this work. The model was validated using measurement data for a class A vehicle in different environmental conditions.

In the prediction function, the external conditions, such as the weather data, the route information, and the vehicle state, are determined and predicted for the planned trip. The predicted signals are then sent to the MPC along with the associated trajectories for the future. The latter is calculated from the current time step until the end of the prediction horizon. For the current executions, a perfect prediction is assumed. This means the actual system behavior does not deviate from the predicted behavior. This simplification is acceptable for the current evaluation of the potential of the functions. However, the effects cannot be neglected in principle [30–32,35]. This still needs to be investigated before the planned vehicle implementation.

The MPC processes the received information and sets up the optimization problem for the current time step using the acados framework [24]. After the optimization is successful, the control signals for the current time step are forwarded to the plant model.

3.2. Modelling of the System Dynamics—Cabin Conditioning

The MPC approach is mainly characterized by the fact that the system behavior is known and can thus be predicted. It follows that modeling the system dynamics is of the highest importance for the quality of the control strategy. On the one hand, the system's behavior must be reflected as accurately as possible; on the other hand, the computing time must be short; otherwise, the real-time capability cannot be guaranteed. In previous publications [19,20], the basic modeling of the cabin conditioning and the special features have already been discussed. For this reason, these shall be briefly summarized. Subsequently, the extension for the consideration of the air humidity is presented.

The overall objective of the model is to determine the heat-up and cool-down behavior of a vehicle cabin and the energy required. For this purpose, a single-zone model of the vehicle cabin was built. The selection of the modeling approach was based on an evaluation of different possibilities. The most complex but accurate way to describe the system characteristics of a vehicle cabin is through a CFD analysis [37,38]. The significant effort required for data processing and the high computing times make it impossible to use in an MPC control strategy. Multi-zone models are the second option for modeling the system behavior. These are mainly used to evaluate the vehicle cabin's energy consumption and calibrate the control approaches. This method also has computing times that cannot meet the real-time criteria for mathematical optimization [39,40]. A disadvantage of this simulation method is that the spatial resolution of the air flows and the temperature distribution cannot be investigated. This also means that more detailed analyses of occupant thermal comfort cannot be carried out. However, these disadvantages can be accepted, as the main purpose of the models is to determine the energy requirements for cabin air conditioning. The statements conclude that the one-zone models are the most suitable of the standard methods for modeling a vehicle cabin using an MPC. A vehicle cabin from an A-segment vehicle with an internal air volume of approximately 2 m^3 was used for this publication. The integrated interior corresponded to that of a basic model in the vehicle series.

The connection of the thermal masses in the interior is characteristic of the heating and cooling behavior of the air inside a vehicle cabin. Due to the chosen modeling approach, it is impossible to differentiate locally between the individual components (for example, steering wheel, dashboard, seats, etc.) in the simulation. For this reason, all thermal masses

of the vehicle cabin are combined into one resulting mass. They are connected to the cabin air via convection with the heat flow $\dot{Q}_{Interior}$. In addition, the total losses via the vehicle shell $\dot{Q}_{Amb}$ and the solar radiation $\dot{Q}_{Solar}$ entering via the window surfaces must also be taken into account in the model. Finally, the incoming and outgoing air mass flow $\dot{m}_{Air,i}$ and the heat flow emitted by the passengers $\dot{Q}_{Pass}$ are accounted for. An overview of the considered boundaries is shown in Figure 2. The validation basis for this model was available measurement data for a class A vehicle.

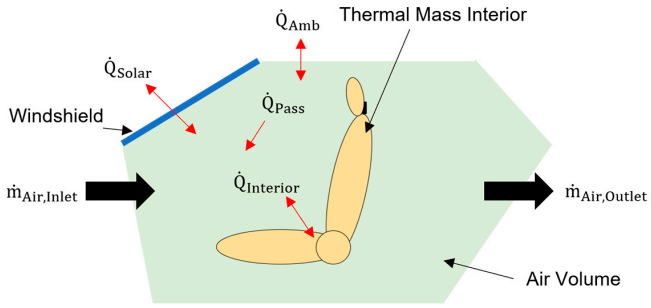

Figure 2. Schematic overview of the simulation model for the air volume of the vehicle cabin.

The representation of the HVAC extended the model. The airflow provided by the HVAC can be taken from the environment (fresh air mode) or the cabin interior (recirculation mode). The user can continuously adjust between the two modes. In addition to the described relationships, the impact of passengers on the cabin in terms of heating and CO_2 production is also considered. The latter influences the air quality. For the investigations in this work, a limit value of 1200 ppm in the interior was selected according to the recommendations in [41]. In the work published, the assumption was made that the air is always dry. For real systems, however, it significantly influences energy demand and comfort [42]. Preventing window fogging is also crucial due to its relevance to safety [21,42]. For this reason, the system modeling was extended by considering air humidity, which is explained in the following section.

In the first step, the state variables for the cabin were extended by modeling the air humidity and the amount of water inside. The water quantities of the incoming and outgoing airflow account for this. In addition, it must be considered that the occupants also emit water into the interior through breathing and sweating. The necessary parameters and formulas were taken directly from [42,43]. The biggest challenge in implementing the humidity was adapting the HVAC model. The active heating and cooling of the airflow directly affects the humidity. For example, cooling the air can cause water to precipitate and thus actively reduce the humidity of the air stream after the subsequent heating [42,43]. The extended functionality of the HVAC model is described in more detail below and visualized in Figure 3.

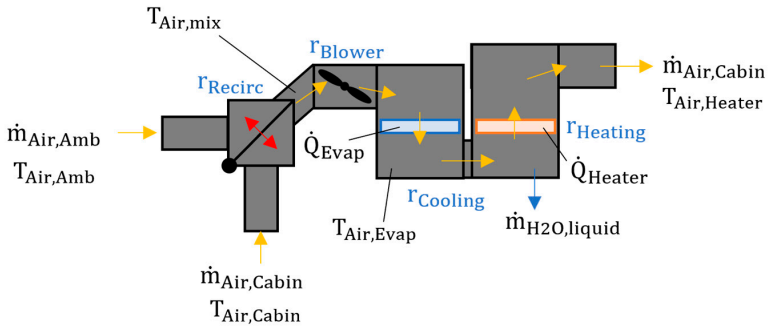

Figure 3. Schematic overview of the simulation model for the HVAC.

The HVAC system determines the conditions of the air entering the cabin. These properties can be adjusted via the control variables, which correspond to each component

within the HVAC system. The summary of all control signals for the HVAC is presented in (6). The airflow itself is provided by a blower fan (~300 W), which is actuated by r_{Blower}. The control values for r_{Cooling} and r_{Heating} determine to which extend the air is heated up or cooled down by the system. The modeled vehicle was equipped with a direct air heater with a maximum output of 5 kW. The compressor within the refrigerant circuit for cooling the cabin has a maximum performance of 8 kW. The last variable r_{Redirect} expresses which proportion of the air flow is redirected from the cabin to the HVAC. If the value is $r_{\text{Redirect}} = 1$, the cabin conditioning is running in recirculation mode. In contrast, a value of $r_{\text{Recirc}} = 0$ indicates a fresh mode operation of the HVAC.

$$u_{\text{HVAC}} = \begin{bmatrix} r_{\text{Blower}} & r_{\text{Recirc}} & r_{\text{Cooling}} & r_{\text{Heating}} \end{bmatrix} \tag{6}$$

For the simplification of the calculations, the relation between the current air mass flow and the control variable is linearized to the following equation:

$$\dot{m} = \dot{m}_{\text{max}} \times r_{\text{Blower}} \tag{7}$$

The value $\dot{m}_{\text{max}}$ is defined as the maximum mass flow the blower can provide. The energy consumption of the blower P_{Blower} is defined by the following equation:

$$P_{\text{Blower}} = P_{\text{Blower,Max}} \times {r_{\text{Blower}}}^2 \tag{8}$$

The relationship between the increased mass flow and energy consumption is quadratic due to the kinetic energy [21].

The airflow provided by the blower consists of a mixture of ambient and cabin air, which is determined by the control variable r_{Recirc}. The calculations used to determine the changes in the temperature of the mixed air flows $T_{\text{Air,mix}}$ as well as the resulting CO_2 concentration $x_{\text{mix,CO}_2}$ and water concentration $x_{\text{mix,H}_2\text{O}}$ are shown below [21].

$$T_{\text{Air,mix}} = \frac{r_{\text{Recirc}} \times c_{\text{p,1+x,Cbn}} \times T_{\text{Air,Cabin}} + (1 - r_{\text{Recirc}}) \times c_{\text{p,1+x,Amb}} \times T_{\text{Air,Amb}}}{r_{\text{Recirc}} \times c_{\text{p,1+x,Cabin}} + (1 - r_{\text{Recirc}}) \times c_{\text{p,1+x,Amb}}} \tag{9}$$

$$x_{\text{mix,H}_2\text{O}} = r_{\text{Recirc}} \times x_{\text{Air,Cabin,H}_2\text{O}} + (1 - r_{\text{Recirc}}) \times x_{\text{Amb,H}_2\text{O}} \tag{10}$$

$$x_{\text{mix,CO}_2} = r_{\text{Recirc}} \times x_{\text{Air,Cabin,CO}_2} + (1 - r_{\text{Recirc}}) \times x_{\text{Amb,CO}_2} \tag{11}$$

The specific heat capacity $c_{\text{p,1+x,i}}$ the heat capacity of humid and the other parameters are determined for either the ambient or the cabin proportion of the air flow [21,43]. All fluid properties for the model were taken from [44] or [45]

In addition, to calculate the values at the evaporator, a distinction was needed between the case with condensation and the case without condensation. Therefore, no direct calculation of the resulting temperature was possible. Instead, in the first step, the enthalpy of the exiting airflow was calculated [43].

$$h_{\text{cool,out}} = h_{\text{cool,in}} - \frac{\dot{H}_{\text{cool,Max}} \times r_{\text{Cooling}}}{\dot{m}} \tag{12}$$

The enthalpy of the entering air $h_{\text{cool,in}}$ is calculated using the following general formula [43].

$$h_i = c_{\text{p,1+x,i}} \times (T_i - T_0) + x_{\text{H}_2\text{O,i}} \times H_0 \tag{13}$$

To determine if condensation occurs within the evaporator, the water load of the incoming stream $x_{\text{H}_2\text{O,in}}$ is compared to the maximal water load at the evaporator outlet $x_{\text{H}_2\text{O,dew}}$ [43].

$$x_{\text{H}_2\text{O,out}} = \begin{cases} x_{\text{H}_2\text{O,in}} & \text{if } x_{\text{H}_2\text{O,in}} < x_{\text{H}_2\text{O,dew}} \\ x_{\text{H}_2\text{O,dew}} & \text{else} \end{cases} \tag{14}$$

Using this relationship, the amount of condensing water can also be calculated. It is assumed that the liquid water $\dot{m}_{H_2O,liquid}$ instantly leaves the system and can therefore not be reabsorbed later [43]. The variable $x_{H_2O,dew}$ is dependent on the enthalpy at the evaporator outlet. Using lookup tables, a function can be fitted to approximate the relationship between $x_{H_2O,dew}$ and $h_{cool,out}$ [21].

$$x_{H_2O,dew} = a_1 \times \exp(-a_2 \times h_{cool,out}) + a_3 + a_4 \times h_{cool,out} \quad (15)$$

The temperature of the airflow leaving the evaporator can now be calculated with Equation (18) [43].

$$T_{Air,Evap} = T_0 + \frac{h_{cool,out} - x_{H_2O,out} \times H_0}{c_{p,1+x,i}} \quad (16)$$

After the evaporator, the airflow enters the heater. The temperature changes within the heater are calculated using Equation (17) [43].

$$T_{Air,Heater} = \frac{\dot{h}_{Heating,Max}}{\dot{m}_{max} \times c_{p,1+x,Heating}} \times r_{Heating} + T_{Air,Evap} \quad (17)$$

The evaporator determines the temperature, the concentrations of CO_2, and the amount of water within the airflow, although they typically do not change during the heating process. The airflow properties entering the cabin can be calculated using these calculations. A typical function of the HVAC, which was not implemented in the model version presented, is an additional mixing chamber after the air heater. Together with an air bypass, this allows unconditioned air to be mixed with conditioned air and then enter the cabin. It represents an additional option for achieving the desired humidity and temperature. However, the elimination of this option does not mean a reduction in possible applications and was not featured in the HVAC system of the selected target vehicle. For future applications, this option can be added at any time.

As mentioned before, window fogging shall be prevented at any time. An obstructed view due to condensation on the windshield is a safety-related issue. Therefore, cabin humidity must be kept below the critical humidity for condensation on the windshield. This limit is calculated based on the windshield's temperature and external boundaries. The windshield temperature must be calculated using an approximation based on the heat flow between cabin air and the ambient [21].

For such an evaluation, the windshield heat transfer must be analyzed. As illustrated in Figure 4, the air flows inside and outside the glass area must be considered. The conductive heat transfer through the glass itself must also be calculated. For the condensation on the inside of the windshield, only the inner surface temperature $T_{Win,Internal}$ is relevant. This temperature can be determined with the following formula [21]:

$$T_{Win,Internal} = \frac{(\alpha_{Win,External} + \lambda_{Win})\alpha_{Win,Internal} T_{Air,Cbn} + \alpha_{Externall} \lambda_{Win} T_{Air,Amb}}{(\alpha_{Win,External} + \lambda_{Win})\alpha_{Win,Internal} + \alpha_{External} \lambda_{Win}} \quad (18)$$

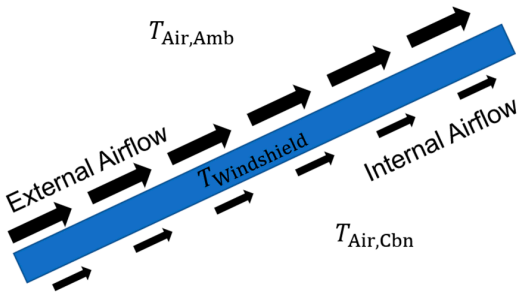

Figure 4. Schematic illustration of the modeling of the windshield temperature.

It uses the conductive heat transfer coefficient for glass λ_{Win} and the convective heat transfer at the outside ($\alpha_{Win,External}$) and the inside ($\alpha_{Win,Internal}$) of the windshield. To include the new variable in the optimization, a state variable for the windshield temperature has to be added to the system dynamics model. After that, the proper boundaries of the connected airflows must be represented. Therefore, ambient and cabin airflows define the air velocities inside and outside the windshield. Balancing the heat transfers between the external and internal air is critical to modeling the temperature of the cabin windshield. Comparing the internal surface temperature to the dew point limits the humidity to a level where window fogging is prevented [21].

A more detailed study of the mechanisms behind windshield fogging by Leriche et al. [46] showed that solar radiation is a significant impact factor. However, the influence of solar radiation is neglected in this first approximation. This is possible without risking unexpected condensation since solar radiation can only result in an increased window temperature compared to no solar radiation. Therefore, solar radiation should be addressed in this part of the model. The correlations of the windshield temperatures lead to a critical humidity value, which is then used as a threshold for the MPC strategy [21].

The methods presented here show some adjustments made to account for humidity. In addition, adaptations to the cost functions and the calibration of the models were also necessary. In the first step, limitations of the cabin air humidity were introduced to prevent window fogging. Therefore, the cost function was extended by a term calculating the difference between the dew point temperature at the current cabin conditions and the introduced internal windshield temperature. The difference is involved in a cost function term and calibrated with a scaling factor. As window fogging is relevant to safety, the scaling factor was initially set to a value that prioritizes humidity reduction quite early. In addition, an offset to the temperature differences between the dew point and the glass surface temperature was implemented to have an extra safety margin.

Furthermore, the model was extended by radiant panel heating. It was already demonstrated in [10] that this can save energy during heating. Therefore, it is necessary to evaluate the interior comfort separately in addition to the air temperature. This was fulfilled by the implementation of the equivalent temperature (EQT). The equivalent temperature can be understood as a theoretical evaluation parameter for thermal comfort in a defined environment. It describes the perception of a room climate, considering the air temperature, the effect of radiation, and the air velocity. This is essential to evaluate the influence of radiant heating on indoor comfort. For this purpose, a mean radiant temperature t_{mr} must first be determined (19) [47]:

$$t_{mr} = \sqrt[4]{(t_{sen} + 273.15)^4 + \frac{h_{Conv}}{\varepsilon \sigma_{SB}}(t_{sen} - t_a) + \frac{m_{sen} c_{p,sen}}{\varepsilon \sigma_{SB} A}\frac{dt}{d\tau}} \tag{19}$$

When determining this value, it is important to use a specific sensor and to have precise knowledge of its properties about radiant (ε) and convective (h_{Conv}) heat transfer. Together with the Stefan–Boltzmann (σ_{SB}) constant, the thermal capacity $(m_{sen}c_{p,sen})$, and the surface area (A), such a value can be calculated [47]. The evaluations in [10] show an example of how such a sensor is constructed and what properties it must have. These findings were used with existing measurement data to transfer this relationship in the simulation model.

To determine the equivalent temperature (20), the air velocity (v_a) inside the cabin and a clothing factor I_{cl} for the virtual occupants are also required. The latter describes how well they are insulated against heat transfer. The numerical values for the clothing factor can be taken from the tables in [48], for example.

$$t_{eq} = 0.55 \times t_a + 0.45 \times t_{mr}\frac{0.24 - 0.75\sqrt{v_a}}{1 + I_{cl}} \times (36.5 - t_a) \tag{20}$$

All necessary correlations can be found in [47–50]. Implementing the equivalent temperature to the system dynamics model can also be utilized for the MPC control strategy; by doing that, the cabin can be conditioned to a targeted perception of the environment instead of a fixed air temperature. For a more detailed description of the modeling, please refer to [19,20].

4. Investigations to Determine the Effectiveness of the MPC Approach

This investigation aims to demonstrate the operation of the MPC with humid air. Both cold and hot ambient conditions were considered. The focus should be on compliance with the fogging limits and the impact of humidity on energy consumption. For this purpose, the MPC was compared with a rule-based strategy. The exact boundary conditions are described below before the results are presented.

4.1. Description of the Rule-Based Control Strategy (RB) Used as the Basis for the Assessment

In [21], an operating strategy was presented based on the current state of the art. It can deal with the CO_2 concentration inside the cabin and adjust the recirculation rate accordingly. This was used as a basis and implemented for the comparison carried out. The principles of operation are briefly summarized in the next section.

In the first step, the airflow is controlled based on the deviation of the current cabin temperature from the desired set point temperature. The smaller the deviation, the lower the actuation of the cabin blower. However, a minimum airflow is always ensured. Reducing the air mass flow when the desired temperature is reached ensures stable control. The baseline control strategy aims to operate the system in recirculation mode as long as possible. It is possible to vary the recirculation rate between 0.1 and 0.9 continuously. The maximum value is maintained until the CO_2 limit of 1200 ppm is reached. From this point on, 90% of the air is drawn from the ambient. This means that the system is in fresh air mode. In this phase, the fan speed is also increased again to improve air quality. After reaching a lower threshold of 600 ppm, the system switches back to recirculation mode and resumes the original fan strategy. A PID control ensures the cooling and heating of the airflow.

4.2. Simulation Results at Cold Ambient Conditions

For cold ambient conditions, a heat-up of the cabin at −10 °C was simulated. For the duration, a period of 3600 s was selected. This equals a drive of two consecutive WLTC cycles. The desired temperature in the cabin was set to 20 °C, and as a target for the CO_2 concentration, 1200 ppm was chosen. A deviation from both target values was penalized by the cost function. The temperature set point was a target value for the equivalent temperature. The radiant heating panels were not activated for this first investigations. As additional ambient conditions, a relative humidity of 0.9 and a solar radiation of 0 W/m^2 were assumed.

Due to the different nature of the MPC and the RB strategy, it is not possible to ensure that the same temperature prevails in the interior at all times during the investigation. Both reached an indoor temperature of 18 °C within a short and comparable time. However, it can be seen that the MPC took longer to overcome the remaining 2 °C to reach the control target. Another aspect that stands out when comparing the temperature signals is that the MPC always remained slightly below the targeted 20 °C (control deviation less than 0.3 °C), while the RB approach sometimes exceeded this. This definitely has an influence on the energy and heating demands for cabin air conditioning. However, due to the small differences over time and the relatively low remaining control deviation of the MPC, this is accepted for this study. In future investigations, however, the cost function could be adjusted to achieve the target temperature more precisely, and additional rule-based comparison strategies could be used for the evaluation.

Figure 5 shows an overview of the control signals for the cabin blower (black), the recirculation rate (red), and the heating (blue). The individual signals are normalized to

their maximum value and given as a percentage. The values of the MPC strategy (MPC) are shown with solid lines and those of the rule-based strategy (RB) with dashed lines. When examining the blower behavior, it is apparent that the RB variant reduces the fan output and therefore the air mass flow earlier, keeping it at a lower level on average. The recirculation rate for RB is almost always at the maximum value of 0.9, except for the phases in which the system switches to fresh air mode to improve air quality. These are also the only phases in which the fan output is increased slightly. In comparison, the MPC keeps the recirculation rate constant at a very high level. The somewhat higher fan speed ensures the required air quality. It can also be seen that the MPC generally requires less heating power. The heating requirement for the RB strategy is significantly higher, particularly during the fresh air operation phases. Similar observations were also made in [51].

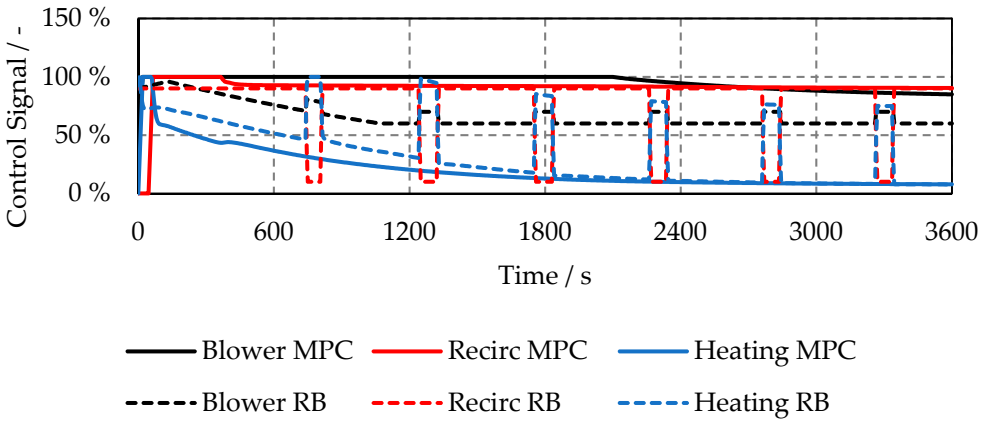

Figure 5. Comparison of the control signals for a cabin heat-up at −10 °C between the MPC and the RB approach.

The control signals' observations are confirmed when analyzing the energy demand for cabin conditioning in Figure 6. It is clear that energy can be saved by using the MPC. Overall, the savings amount to approximately 15.4%. Although more energy is invested in the fan's operation and thus in an increased air mass flow, significant benefits can be achieved by reducing the cooling requirement.

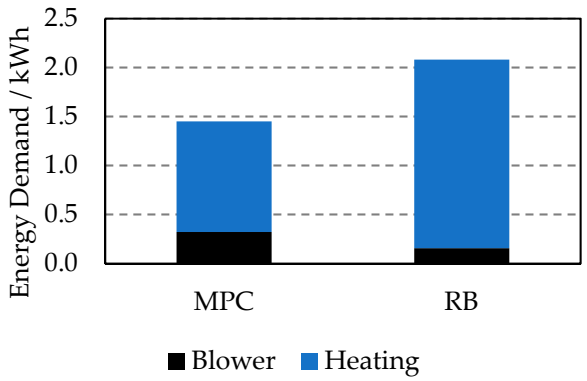

Figure 6. Comparison of the energy demand for a cabin heat-up at −10 °C between the MPC and the RB approach.

Figure 7 shows the CO_2 concentration curves inside the cabin for both strategies. The limit (red) can be adhered to by the MPC (blue) and the RB variant (black) for the majority of the scenario. When the recirculation rate (Figure 5) and the CO_2 concentration (Figure 7) for RB and the MPC are compared, the difference between the two approaches becomes clear. The maximum for the recirculation rate of the MPC is not limited to 0.9 and goes up to 1. The CO_2 concentration at the start rose faster due to the higher recirculation than the rule-based approach. After the limit of 1200 ppm was exceeded, the recirculation rate

remained high for a certain period. After that, the MPC slowly reduced it to fall below the limit again. The MPC valued the energy costs at the beginning of the heat-up process higher than maintaining the CO_2 limits. This could be adapted by changing the cost function to meet higher requirements for air quality. Nevertheless, this is not considered efficient, as a slide overrun of the threshold should be classified as not critical for the passengers [41,52]. The CO_2 level for the rule-based approach increased much slower due to the maximum recirculation rate of 0.9. The fresh air mode was activated as soon as the limit was reached. The process was repeated multiple times during the simulation.

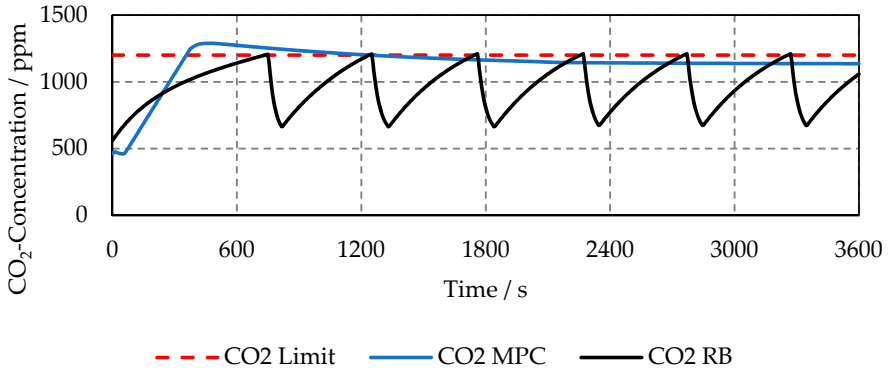

Figure 7. Comparison of the CO_2 concentration for a cabin heat-up at −10 °C between the MPC and the RB approach.

Due to the low response time of the electric air heaters, the air entering the cabin was already quite dry at the start of the simulation. Therefore, the humidity remained below the threshold value, indicating the risk of windshield fogging. In both cases, the humidity in the cabin was reduced quickly. Therefore, no other actions have to be considered. In other use cases, it could be observed that the MPC uses active dehumidification to stay below the humidity threshold. This method is very energy-intensive and only used when other measures cannot prevent window fogging. The results can also be seen in Figure 8. It can be noted that the humidity for the MPC application was slightly lower at the beginning of the simulation. This can be explained by the rule-based approach, obtaining 10% of the airflow from the environment at the start. The ambient humidity was very high. Therefore, the humidity inside the cabin also remained higher at this time. This effect could be neglected if the upper limit for the rule-based approach could also be set to 1. For more critical boundary conditions, this could lead to an increased risk of windshield fogging.

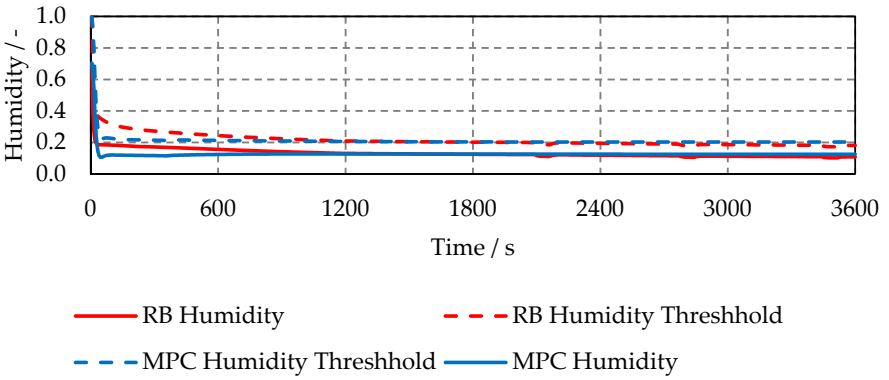

Figure 8. Humidity inside the cabin and upper humidity limit for a cabin heat-up at −10 °C.

4.3. Simulation Results at Hot Ambient Conditions

For hot conditions, an ambient temperature of 35 °C, relative humidity of 0.4, and solar radiation of 800 W/m^2 were chosen. All additional settings and boundaries were kept unchanged compared to the cold conditions. Once again, both control approaches could

condition the cabin to the desired target temperature comparably quickly. The average control deviation required was below 0.3 °C for both methods. The differences between the indoor temperatures during the conditioning phase can also be identified for the hot scenario. However, these are even smaller than in the heating operation and are therefore also accepted for this publication.

Figure 9 shows the control signals for the control-based approach (RB) and the MPC for the cabin cooling process at 35 °C outside temperature. Similar to the cabin's heating, it is clear that the MPC approach used a higher fan speed. However, this was accompanied by a constantly higher recirculation rate, resulting in a lower power requirement for cabin cooling. Once again, it is noticeable that the cooling demand for RB rose sharply during the fresh air operation phase. As these tended to become longer in the course of the simulation, they had a significant effect on the system behavior.

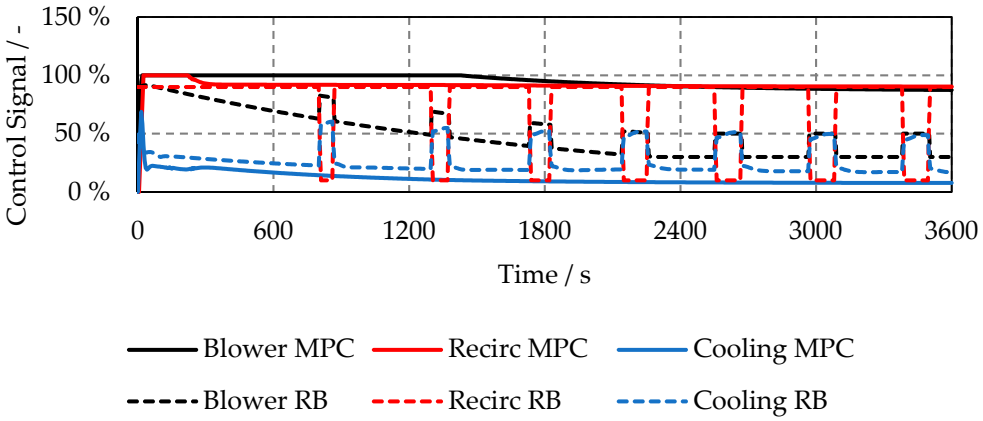

Figure 9. Comparison of the control signals for a cabin cool-down at 35 °C between the MPC and the RB approach.

This is also reflected in the energy demands for cabin air conditioning, illustrated in Figure 10. The MPC also used an increased air mass flow and a higher average recirculation rate for hot ambient temperatures to reduce the energy requirement. The simulation identified a savings potential of 37.9%.

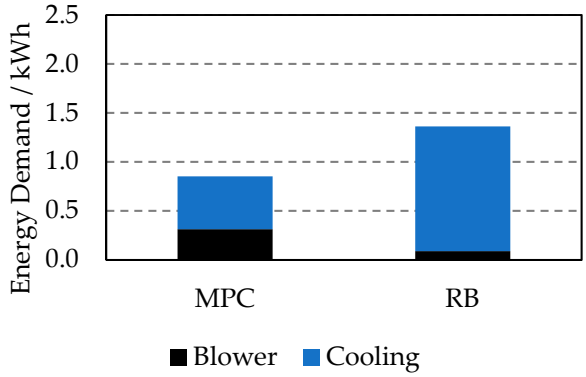

Figure 10. Comparison of the energy demand for a cabin cool-down at 35 °C between the MPC and the RB approach.

Figure 11 shows the CO_2 concentration for the MPC (blue) and the rule-based approach (black) in comparison to the limitation (red). Observing the CO_2 concentration and the respective recirculation rates presented in Figure 9, it becomes evident that the rule-based approach is forced to switch to fresh air mode more often than for cold conditions. This is an additional reason for the additional energy demand for the cabin's heating. Nevertheless, both strategies are capable of maintaining the limitation for the air quality at any time.

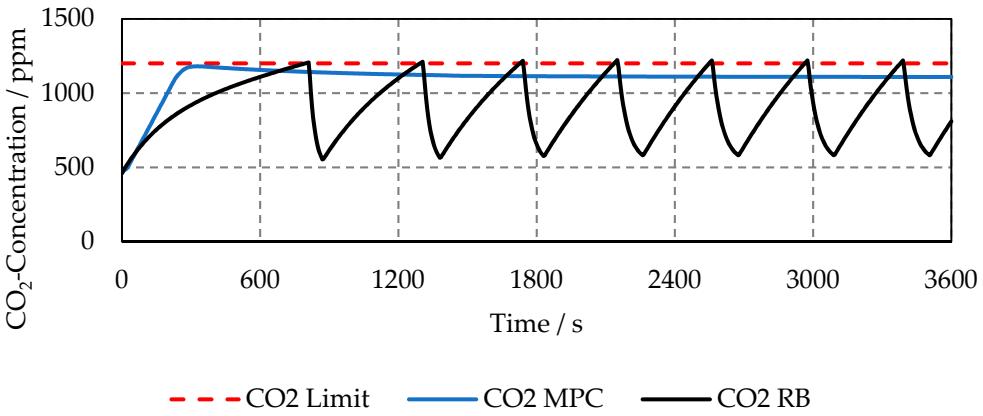

Figure 11. Comparison of the CO_2 concentration for a cabin cool-down at 35 °C between the MPC and the RB approach.

When looking at the humidity (Figure 12), the threshold values for preventing windshield fogging cannot be seen, as they are higher than 1. This seems unconvincing at first sight, as the relative humidity is limited to 1. The values must be interpreted as a theoretical representation of the limit value. It symbolizes that the humidity must theoretically exceed one at the given windshield temperature to cause window fogging. That means it is practically impossible to have window fogging at this status because of the high windshield temperature. In addition, it can be observed that the humidity inside the cabin increases every time the fresh air mode is engaged. Although this does not impact the windshield fogging for the investigated use case, it could be an issue for scenarios with more passengers or critical ambient conditions.

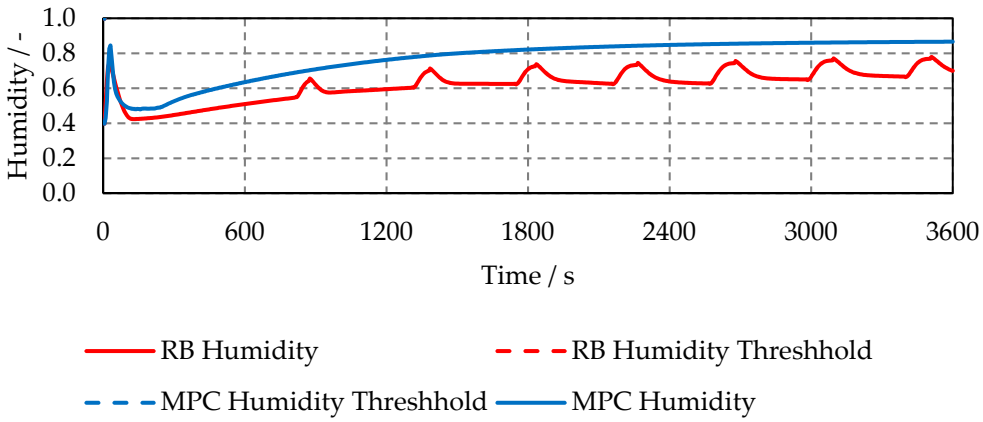

Figure 12. Humidity inside the cabin and upper humidity limit for a cabin cool-down at 35 °C.

5. Summary and Outlook

This paper presented a model predictive approach for the cabin conditioning of BEVs. The focus was on considering the air humidity in the control strategy and preventing windshield fogging. The necessary steps to change the existing system dynamics model were explained. The changes to the calculations within the air path and the implementation of the windshield area as an indication of the risk for window fogging were discussed in detail. It was shown that it is possible to include the air humidity appropriately and thus add a safety level for optimizing the control strategy for cabin conditioning. Also, the impact of air humidity on the energy demand was examined. In the presented MiL investigations, energy-saving potentials of up to 15.4% for cold and 37.9% for hot ambient conditions were achieved.

The presented findings show that the use of an MPC control strategy has a positive effect on the energy consumption of the cabin air conditioning and the thermal comfort in

the passenger compartment. By using external information sources for the control strategies, future BEVs can benefit from the growing connectivity. Particularly in the important area of thermal management, MPC strategies can generate an increase in driving range, which can contribute to improving the acceptance of electric mobility.

Future studies should therefore be extended to other areas of thermal management, such as battery conditioning or the operation of complex heat pumps, in order to identify further energy-saving potential. The growing possibilities for creating powerful and fast-calculating models through the advance of machine learning and other methods could be further levers for potentiating the effectiveness of MPC in the future.

Author Contributions: Conceptualization, P.S. and P.H.; methodology, P.S. and P.H.; software, P.S. and P.H.; validation, P.S., K.F. and P.H.; formal analysis, P.S., S.P., D.H., K.F. and P.H.; investigation, P.S., K.F. and P.H.; resources, P.S., K.F. and P.H.; data curation, P.S.; writing—original draft preparation, P.S. and P.H.; writing—review and editing, P.S., S.P., D.H., K.F. and P.H.; visualization, P.S. and K.F.; supervision, S.P. and D.H.; project administration, P.S. and D.H.; funding acquisition, P.S., S.P. and D.H. All authors have read and agreed to the published version of the manuscript.

Funding: This project has received funding from the European Union's Horizon 2020 research and innovation programme under grant agreement 628 No 824295.

Data Availability Statement: The original contributions presented in the study are included in the article, further inquiries can be directed to the corresponding author.

Conflicts of Interest: David Hemkemeyer is employee of FEV Europe GmbH. The paper reflects the views of the scientists, and not the company.

References

1. Bundesministerium für Wirtschaft und Klimaschutz: Abkommen von Paris. Available online: https://www.bmwk.de/Redaktion/DE/Artikel/Industrie/klimaschutz-abkommen-von-paris.html (accessed on 29 February 2024).
2. Europäische Kommission. Umsetzung des europäischen Grünen Deals: Auf dem Weg zu einem Klimaneutralen Europa bis 2050. Available online: https://commission.europa.eu/strategy-and-policy/priorities-2019-2024/european-green-deal/delivering-european-green-deal_de (accessed on 29 February 2024).
3. Bundesregierung. Klimaschutzgesetz: Generationenvertrag für das Klima. 7 November 2022. Available online: https://www.bundesregierung.de/breg-de/schwerpunkte/klimaschutz/klimaschutzgesetz-2021-1913672 (accessed on 29 February 2024).
4. Europäische Kommission. Special Eurobarometer 513—Climate Change: Report. Available online: https://ec.europa.eu/clima/system/files/2021-07/report_2021_en.pdf (accessed on 29 February 2024).
5. Europäische Kommission. Mitteilung der Kommission an das Europäische Parlament, den Rat, den Europäischen Wirtschafts- und Sozialausschuss und den Ausschuss der Regionen: „Fit für 55": Auf dem Weg zur Klimaneutralität—Umsetzung des EU-Klimaziels für 2030. Available online: https://eur-lex.europa.eu/legal-content/DE/TXT/PDF/?uri=CELEX:52021DC0550&from=DE (accessed on 29 February 2024).
6. Bundesregierung. Nachhaltige Mobilität: Nicht Weniger Fortbewegen, Sondern Anders. 23 December 2022. Available online: https://www.bundesregierung.de/breg-de/schwerpunkte/klimaschutz/nachhaltige-mobilitaet-2044132 (accessed on 29 February 2024).
7. European Environment Agency. New Registrations of Electric Vehicles in Europe. Available online: https://www.eea.europa.eu/ims/new-registrations-of-electric-vehicles (accessed on 29 February 2024).
8. Götz, K.; Sunderer, G.; Birzle-Harder, B.; Deffner, J. *Attraktivität und Akzeptanz von Elektroautos: Ergebnisse aus dem Projekt OPTUM. Optimierung der Umweltentlastungspotenziale von Elektrofahrzeugen*; ISOE: Frankfurt am Main, Germany, 2012.
9. Tschöke, H.; Gutzmer, P.; Pfund, T. *Elektrifizierung des Antriebsstrangs: Grundlagen—Vom Mikro-Hybrid zum vollelektrischen Antrieb*; ATZ/MTZ-Fachbuch; Springer: Berlin/Heidelberg, Germany, 2019.
10. Hemkemeyer, D. Thermomanagement im Elektrischen Personenkraftwagen unter Nutzung der Abwärme des Antriebs. Ph.D. Thesis, RWTH Aachen University, Aachen, Germany, 9 October 2017.
11. Beetz, K.; Kohle, U.; Eberspach, G. Beheizungskonzepte für Fahrzeuge mit Alternativen Antrieben. *ATZ Automob. Z.* **2010**, *112*, 246–249. [CrossRef]
12. Allgemeiner Deutscher Automobil-Club E.V. Stromverbrauch von Sitzheizung und Co: Wie Hoch ist er Tatsächlich? Available online: https://www.adac.de/rund-ums-fahrzeug/ausstattung-technik-zubehoer/ausstattung/sitzheizung-verbrauch/ (accessed on 29 February 2024).
13. Rudschies, W. Elektroauto im Winter: So wirkt sich Kälte auf Verbrauch und Reichweite aus. Available online: https://www.adac.de/rund-ums-fahrzeug/elektromobilitaet/info/elektroauto-reichweite-winter/ (accessed on 29 February 2024).

14. Auer, M. *Ein Beitrag zur Erhöhung der Reichweite eines Batterieelektrischen Fahrzeugs durch Prädiktives Thermomanagement*; Springer: Wiesbaden, Germany, 2016.
15. VDI und VDE. Brennstoffzellen- und Batteriefahrzeuge: Bedeutung für die Elektromobilität. Last Updated: 7 June 2019. Available online: https://www.vdi.de/ueber-uns/presse/publikationen/details/brennstoffzellen-und-batteriefahrzeuge (accessed on 27 April 2022).
16. Chen, Y.; Kwak, K.H.; Kim, J.; Kim, Y.; Jung, D. Energy-efficient cabin climate control of electric vehicles using linear time-varying model predictive control. *Optim. Control Appl. Methods* **2023**, *44*, 773–797. [CrossRef]
17. Wang, H.; Meng, Y.; Zhang, Q.; Amini, M.R.; Kolmanovsky, I.; Sun, J.; Jennings, M. MPC-based Precision Cooling Strategy (PCS) for Efficient Thermal Management of Automotive Air Conditioning System. In Proceedings of the 2019 IEEE Conference on Control Technology and Applications (CCTA), Hong Kong, China, 19–21 August 2019; pp. 573–578.
18. Liu, Y.; Zhang, J. Electric Vehicle Battery Thermal and Cabin Climate Management Based on Model Predictive Control. *J. Mech. Des.* **2021**, *143*, 031705. [CrossRef]
19. Manns, P.; Hemkemeyer, D.; Linse, D. Predictive Cabin Climatization for Electric Vehicles. *ATZ Worldw.* **2022**, *124*, 36–39. [CrossRef]
20. Schutzeich, P.; Pischinger, S.; Hemkemeyer, D.; Wahl, A.; Franke, K. A Model Predictive Control Strategy for Advanced Passenger Compartment Air Conditioning in Vehicles with Electrified Powertrains. In Proceedings of the 2022 SAE Thermal Management Systems Symposium, Plymouth, MI, USA, 4–5 October 2022.
21. Schaut, S.; Sawodny, O. Thermal Management for the Cabin of a Battery Electric Vehicle Considering Passengers' Comfort. *IEEE Trans. Control Syst. Technol.* **2020**, *28*, 1476–1492. [CrossRef]
22. Verschueren, R.; Frison, G.; Kouzoupis, D.; Frey, J.; Van Duijkeren, N.; Zanelli, A.; Novoselnik, B.; Albin, T.; Quirynen, R.; Diehl, M. acados—A modular open-source framework for fast embedded optimal control. *Math. Program. Comput.* **2022**, *14*, 147–183. [CrossRef]
23. Systems Control And Optimization Laboratory. acados—Documentation. Last Updated: 2 January 2024. Available online: https://docs.acados.org/ (accessed on 29 February 2024).
24. Systems Control And Optimization Laboratory. acados—Embedded Workflow. Available online: https://docs.acados.org/embedded_workflow/index.html (accessed on 29 February 2024).
25. Cevolver Project Consortium. CEVOLVER: Connected Electric Vehicle Optimized for Life, Value, Efficiency and Range. Available online: https://cevolver.eu/ (accessed on 29 February 2024).
26. Cevolver Project Consortium. Integrated Energy & Thermal Management Validator: Poster. Available online: https://cevolver.eu/wp-content/uploads/2022/10/CEVOLVER_Poster_Validator1_FINAL.pdf (accessed on 29 February 2024).
27. Schutzeich, P.; Wahl, A. CEVOLVER—Thermal Management Improvements: Poster. Available online: https://cevolver.eu/wp-content/uploads/2022/10/CEVOLVER_Final_Event_Poster_Thermal_Management_FINAL.pdf (accessed on 29 February 2024).
28. Wahl, A.; Schutzeich, P. CEVOLVER—Advanced Thermal Management: An Enabler of Long Distance Capabilities? Available online: https://cevolver.eu/wp-content/uploads/2022/10/Thermal_Management_in_CEVOLVER_Final_Event_V8_compressed.pdf (accessed on 29 February 2024).
29. Schutzeich, P.; Hemkemeyer, D.; Franke, K.; Hamelbeck, P. A Predictive Cabin Conditioning Strategy for Battery Electric Vehicles. 36th International Electric Vehicle Symposium and Exhibition (EVS36). Available online: https://evs36.com/wp-content/uploads/finalpapers/FinalPaper_Schutzeich_Patrick.pdf (accessed on 13 December 2023).
30. Papageorgiou, M.; Leibold, M.; Buss, M. *Optimierung: Statische, Dynamische, Stochastische Verfahren für die Anwendung*; Springer: Berlin/Heidelberg, Germany, 2015; pp. 343–427.
31. Adamy, J. *Nichtlineare Systeme und Regelungen*; Springer: Berlin/Heidelberg, Germany, 2018; pp. 227–280.
32. Schwarzkopf, S. Echtzeitfähige Optimierungsbasierte Regelung von Stofftrennprozessen. Magdeburg, Otto-von-Guericke-Universität Magdeburg, Fakultät fur Elektrotechnik und Informationstechnik. Dissertation. 16 October 2012. Available online: https://d-nb.info/1054135266/34 (accessed on 24 January 2023).
33. Völz, A. *Modellprädiktive Regelung Nichtlinearer Systeme mit Unsicherheiten*; Springer: Wiesbaden, Germany, 2016.
34. Diehl, M.; Bock, H.G.; Schlöder, J.P. A Real-Time Iteration Scheme for Nonlinear Optimization in Optimal Feedback Control. *SIAM J. Control Optim.* **2005**, *43*, 1714–1736. [CrossRef]
35. Graichen, K. Methoden der Optimierung und optimalen Steuerung: Skriptum (Wintersemester 2012/2013). Last Updated: 5 August 2019. Available online: https://vdocuments.site/skriptum-methoden-der-optimierung-und-optimalen-steuerung-c-prof-dr-ing.html?page=1 (accessed on 25 January 2023).
36. Wahl, A.; Wellmann, C.; Krautwig, B.; Manns, P.; Chen, B.; Schernus, C.; Andert, J. Efficiency Increase through Model Predictive Thermal Control of Electric Vehicle Powertrains. *Energies* **2022**, *15*, 1476. [CrossRef]
37. Danca, P.; Bode, F.; Nastase, I.; Meslem, A. CFD simulation of a cabin thermal environment with and without human body—Thermal comfort evaluation. *E3S Web Conf.* **2018**, *32*, 1018. [CrossRef]
38. Chang, T.-B.; Sheu, J.-J.; Huang, J.-W.; Lin, Y.-S.; Chang, C.-C. Development of a CFD model for simulating vehicle cabin indoor air quality. *Transp. Res. Part D Transp. Environ.* **2018**, *62*, 433–440. [CrossRef]
39. Pathuri, R.; Patil, Y.; Nagarhalli, P.V. Deployment of 1D Simulation with Multi Air Zone Cabin Model for Air Conditioning System Development for Passenger Car. SAE Technical Paper Series. In Proceedings of the Symposium on International Automotive Technology 2015, Warrendale, PA, USA, 21–24 January 2015.

40. Poovendran, K.; Abel, D.; Reuscher, T.; Govender, V. Vehicle Cabin Thermal Multi-Zone Modelling for Control. In Proceedings of the 2020 2nd International Conference on Control Systems, Mathematical Modeling, Automation and Energy Efficiency (SUMMA), Lipetsk, Russia, 11–13 November 2020; pp. 489–495.
41. Angelova, R.A.; Markov, D.G.; Simova, I.; Velichkova, R.; Stankov, P. Accumulation of metabolic carbon dioxide (CO_2) in a vehicle cabin. *IOP Conf. Ser. Mater. Sci. Eng.* **2019**, *664*, 12010. [CrossRef]
42. Großmann, H.; Böttcher, C. *Pkw-Klimatisierung: Physikalische Grundlagen und Technische Umsetzung*; Springer: Berlin/Heidelberg, Germany, 2020.
43. Lucas, K. *Thermodynamik*; Springer: Berlin/Heidelberg, Germany, 2008.
44. Kretzschmar, H.-J.; Wagner, W. D2.1 Thermophysikalische Stoffwerte von Wasser. In *VDI-Wärmeatlas*; Stephan, P., Kabelac, S., Kind, M., Mewes, D., Schaber, K., Wetzel, T., Eds.; Springer: Berlin/Heidelberg, Germany, 2019; pp. 201–218.
45. Ingenieure, V.D. *VDI-Wärmeatlas*; Springer: Berlin/Heidelberg, Germany, 2013.
46. Leriche, M.; Roessner, W.; Reister, H.; Weigand, B. Numerical Investigation of Droplets Condensation on a Windshield: Prediction of Fogging Behavior. SAE Technical Paper Series. In Proceedings of the SAE 2015 World Congress & Exhibition, Detroit, MI, USA, 21–23 April 2015.
47. *DIN EN ISO 14505-2:2007-04*; Ergonomie der Thermischen Umgebung_-Beurteilung der Thermischen Umgebung in Fahrzeugen_-Teil_2: Bestimmung der Äquivalenttemperatur (ISO_14505-2:2006); German Version EN_ISO_14505-2:2006. ISO: Geneva, Switzerland, 2007.
48. Ye, G.; Yang, C.; Chen, Y.; Li, Y. A new approach for measuring predicted mean vote (PMV) and standard effective temperature (SET∗). *Build. Environ.* **2003**, *38*, 33–44. [CrossRef]
49. Shaw, E.W. Thermal Comfort: Analysis and applications in environmental engineering, by P. O. Fanger. 244 pp. DANISH TECHNICAL PRESS. Copenhagen, Denmark, 1970. Danish Kr. 76, 50. *R. Soc. Health J.* **1972**, *92*, 164. [CrossRef]
50. *ANSI/ASHRAE Standard 55-2023*; Thermal Environmental Conditions for Human Occupancy. American Society of Heating, Refrigerating and Air-Conditioning Engineers, Inc., American National Standards Institute: Peachtree Corners, GA, USA, 2023.
51. Arndt, M.; Sauer, M.; Wolz, M. Verbrauchssenkung durch verbesserte Klimaanlagen-Regelung. *ATZ Automob. Z.* **2017**, *109*, 404–410. [CrossRef]
52. Zhang, X.; Wargocki, P.; Lian, Z.; Thyregod, C. Effects of exposure to carbon dioxide and bioeffluents on perceived air quality, self-assessed acute health symptoms, and cognitive performance. *Indoor Air* **2017**, *27*, 47–64. [CrossRef] [PubMed]